Journal of Zhejiang University SCIENCE A
ISSN 1673-565X (Print); ISSN 1862-1775 (Online)
www.zju.edu.cn/jzus; www.springerlink.com
E-mail: jzus@zju.edu.cn

New method of improving parts accuracy by adding heat balance support in selective laser sintering*

Bing LIU, Li-chao ZHANG†‡, Jian-hua MO, Bo QIAN

(*State Key Laboratory of Plastic Forming Simulation and Die and Mould Technology, School of Material Science and Engineering, Huazhong University of Science and Technology, Wuhan 430074, China*)

†E-mail: dr.teac@gmail.com

Received Mar. 26, 2008; Revision accepted July 3; Crosschecked Dec. 29, 2008

Abstract: In order to improve parts accuracy, a method of adding heat balance support (HBS) was proposed, and the detailed algorithm for generating HBS was developed. A number of experiments and a comparison between similar softwares, showed that the algorithm is efficient and feasible. Moreover, different features of HBS were studied for different kinds of materials, such as PS and nylon. The research findings indicate that automatically adding HBS can significantly improve the accuracy of the parts, and that the algorithm for generating HBS is efficient and precise.

Key words: Selective laser sintering (SLS), Accuracy, Heat balance support (HBS), Triangular facet, 3D rings
doi:10.1631/jzus.A0820226 **Document code:** A **CLC number:** TP319

INTRODUCTION

Rapid prototyping (RP) is a technique for the direct conversion of 3D CAD data into a physical prototype using a number of techniques, mostly based on slicing a computer model of a 3D object into multiple 2D layers and building them up, one layer at a time. Industries have been using RP increasingly to reduce their product development cycles. Having realized the potential of RP for prototyping applications, a large number of processes have been developed, allowing the use of various materials ranging from plastics to metals for the development of prototypes (Exner *et al.*, 2008). Selective laser sintering (SLS), invented at the University of Texas at Austin in 1988, has become one of the most effective and versatile RP methods available today (Chua *et al.*, 1998; Kochan *et al.*, 1999). Although SLS can produce objects of any complexity in theory, problems, such as shrinkage and distortion of parts, still occur frequently during processing, which largely limits the application of SLS.

Much research has been devoted to the study of shrinkage and accuracy of the SLS parts. Williams (1998) studied the energy delivery, heat transfer, and sintering process along with other pertinent phenomena. Yang *et al.*(2002) studied the shrinkage compensation of SLS using the Taguchi method. Armillotta (2001) analyzed how layer thickness and part orientation affect surface finish with a graphical simulation technique. Hardro *et al.*(1998) determined the optimal processing parameters of SLS by experiments on elastomeric polymer. Wang *et al.*(2007) applied approaches using neural networks to the study of SLS processing. Du *et al.*(2007) presented a linear drive system that implements the high-accuracy reciprocating motion of the dynamic focus module in SLS RP manufacturing. Laser power, laser scan spacing, powder bed temperature and a dynamic focus system (Ang *et al.*, 2000; Qi *et al.*, 2004; Majewski *et al.*, 2007) are all factors that influence the accuracy of SLS parts. Previous investigations

‡ Corresponding author
* Project supported by the Innovatory Group Program of the Natural Science Foundation of Hubei Province (No. 2004ABC001), and the Open Foundation of State Key Laboratory of Powder Metallurgy of Center South University (No. 200506123102A), China

(Maeda and Childs, 2004; Kolossov *et al*., 2004; Dai and Shaw, 2004; Ming and Gibson, 2006) showed that the thermal imbalance in SLS parts arising in the build chamber during the sintering process was one of the major factors causing shrinkage and poor dimensional accuracy. Therefore, the investigation described in this study has focused on an analysis of the thermal imbalance, and led to a proposal for a way of improving the accuracy of SLS parts.

ANALYSIS AND METHOD

Shrinkage and distortion analysis in SLS processing

The normal preheating temperature is usually maintained 40 or 50 °C below the melting temperature of the semi-crystalline polymer, which can probably preheat the powders and does not make them cake together. When the sintering begins in SLS, the preheating temperature of the powder bed is usually 20 or 30 °C above the normal preheating temperature and it is maintained around 10 or 20 °C below the melting temperature of the semi-crystalline polymer. This is because the high preheating temperature may result in a tendency to powder caking, and the temperature of the powders does not need to be significantly raised when the powders are sintered to the part by laser, reducing the contraction of the powders and preventing the part from warping and distorting. After the processing of four or five layers, the preheating temperature must be dropped to the normal preheating temperature. Otherwise, the sintered part and the powders will stick together firmly, and the processing will be a failure. There are two main preheating sources while processing. The first one is obtained from heating elements in a work-cylinder; The second one comes from laser sintering, that is the region sintered by the laser will have a higher temperature, which plays a role in preheating for the next layer's sintering, also known as bottom heating. The regions of bottom heating provided by laser sintering are confined to the previous sintered regions. If the sintering area of the current layer increases suddenly during processing, that is some sections of the current layer emerge in the external regions of the previous sintered area, these sections will have no bottom heating and this results in a remarkably non-uniform temperature field. If the machine continues to process the part in this situation, shrinkage and warpage will occur to the current layer. In serious cases, the warped regions may be destroyed by the powder spreading device, which will lead to an unfinished work.

Methods of preventing shrinkage and distortion in SLS processing

SLS technology is well known for the production of parts with complex shapes like the ones shown in Fig.1. However, by traditional methods many positions of the part are not heated well from the bottom during the processing, so it is very difficult to ensure its accuracy and quality. A part with some components oriented in the way shown in Fig.1b, which receives no bottom heating, may not be well processed, as shown in Fig.2. In order to improve the uniformity of the temperature field and process a part with high accuracy, it may be an option for layers without bottom heating to be processed in the same way as the processing at the beginning:

(1) Stop manufacturing and set the preheating temperature about 20 or 30 °C above the normal preheating temperature;

(2) Manufacture the part with about four or five

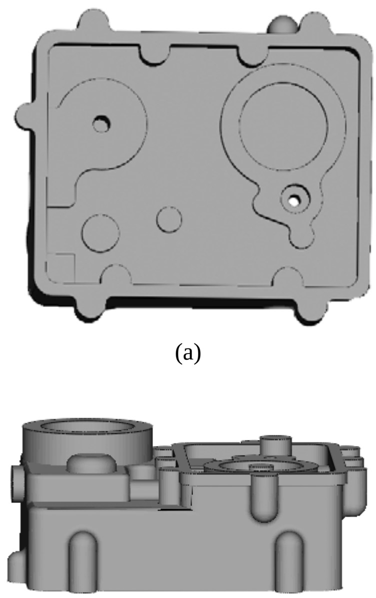

(a)

(b)

Fig.1 Part with sudden increasing area outside the sintered area. (a) Bottom view; (b) Front view

Fig.2 Failed processed part

layers at the improved preheating temperature;

(3) Continue to manufacture the part and synchronously drop the preheating temperature to the normal preheating temperature.

This kind of processing method can improve the accuracy of the part. However, it requires frequent heating and cooling. What is worse, the high preheating temperature can make the powders stick to the processed part, which will cause much difficulty for the purifier to clean the part and may even damage the part.

In order to improve parts accuracy, regions without bottom heating can be supplied with laser sintering. The way to supply bottom heating is to slightly sinter the powders in the regions that need bottom heating before processing, so that the slightly sintered region can supply bottom heating for further processing. Some researchers tried to add support when processing an SLS part so that the support region can supply bottom heating. However, for the parts with large scales and complex shapes it takes much more time to generate supports and to process the supports region. It is more reasonable that this kind of bottom heating is added several layers before processing instead of being added from the bottom of the part. Moreover, the style of the bottom heating may be changeable for different materials. Similar to appending support to the area that needs bottom heating, this type of supplement is therefore defined as heat balance support (HBS). An accurate and efficient algorithm for generating HBS will be described in the next section.

ALGORITHM

The universal data format in the field of RP is STL (Chua *et al*., 2002). An STL format model is composed of a series of connected triangular facets. Before generating HBS, the topology of the STL file must be reconstructed to establish the positional relations of triangular facets, so it is easy to identify adjacent triangular facets (Guo *et al.*, 2007). In accordance with the rules of the composition of STL format, the unit vectors of the triangular facets in the area that need HBS should be either pointing down along the *Z*-axis or at an angle θ to it, as shown in Fig.3. According to the principle of HBS, when the angle θ is greater than a certain value, the triangular facet will need HBS.

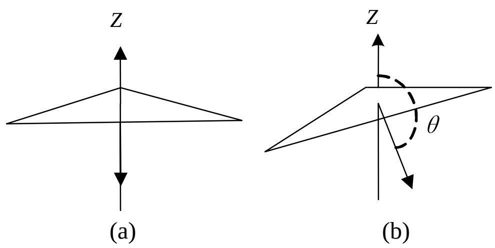

Fig.3 Triangular facets of STL file that need HBS. (a) Vertical downward unit vector; (b) Unit vector at an angle θ to *Z*-axis

The normal of a particular triangular facet is defined as $\boldsymbol{n}$, and $\boldsymbol{k}$ is the unit vector of the *Z*-axis with the equation of "$\boldsymbol{k}$=[0,0,1]"; the dot product between the two vectors is as follows:

$$\boldsymbol{n}\cdot\boldsymbol{k}=|\boldsymbol{n}|\cdot|\boldsymbol{k}|\cdot\cos\theta.$$

Different kinds of planes have different values:

(1) $\boldsymbol{n}\cdot\boldsymbol{k}=0$ ($\theta=90°$), vertical plane;

(2) $\boldsymbol{n}\cdot\boldsymbol{k}=1$ ($\theta=0°$), upward plane;

(3) $\boldsymbol{n}\cdot\boldsymbol{k}=-1$ ($\theta=180°$), downward plane;

(4) $0<\boldsymbol{n}\cdot\boldsymbol{k}<1$ ($\theta<90°$), upward slope;

(5) $-1<\boldsymbol{n}\cdot\boldsymbol{k}<0$ ($\theta>90°$), downward slope.

The set of all triangular facets of an STL model is defined as FACE, and the normal vector of a particular triangular facet in FACE is defined as $\boldsymbol{N}_i$ ($\boldsymbol{N}_1$, $\boldsymbol{N}_2$, …, $\boldsymbol{N}_n$). The dot product between the normal vector of every triangular facet and the unit vector of the *Z*-axis must be calculated. If the triangular facet complies with the following qualification: $-1\le \boldsymbol{N}_i\cdot\boldsymbol{k}<-\cos\theta_k$ (θ_k is the critical angle), place it into DTRIGNGLE which is a set of downward normal vectors, so all triangular facets which need HBSs can be extracted.

When F_i is a certain triangular facet in SF (F_1, F_2,…,F_i,…,F_k,…,F_n are all triangular facets in SF; $1\leq i\leq k\leq n$) which is a set of all triangular facets of an HBS region, a certain triangular facet F_k with the same border as F_i can certainly be found. In order to generate an HBS, the triangular facets in SF must first be divided into different 3D rings. In this study a ring is a set of ordered points, which are composed of the apexes of many triangular facets. These points constitute an array whose starting point connects to the end point. The ring must satisfy the following conditions:

(1) Borders (the line that connects two adjacent points is defined as border) of the ring cannot intersect with each other;

(2) If the ring follows a clockwise direction and the entity is on the left, the ring is an inner-ring. On the contrary, if the ring follows a clockwise direction but the entity is on the right, the ring is an outer-ring.

The generation of rings follows the four steps below:

(1) Randomly extract one triangular facet T_i from DTRIGNGLE (T_1, T_2, ..., T_n are all triangular facets in DTRIGNGLE; $1\leq i\leq n$), which is a set of triangular facets to be added with HBS, then initialize a 3D ring, which is defined as RING and constructed by the three apexes of T_i in anti-clockwise order, and remove T_i from DTRIGNGLE;

(2) Find the triangular facet with the same border as RING from DTRIGNGLE, then remove this border from RING and add the different borders into RING (i.e., add points of certain borders into the ring) in anti-clockwise order;

(3) Repeat Step (2) until the triangular facet with the same border as RING cannot be found in DTRIGNGLE;

(4) Repeat Steps (1)~(3) until DTRIGNGLE is empty.

Fig.4 illustrates a ring constructed by three apexes of a triangular facet in anti-clockwise order. The steps are as follows:

(1) Initialize a ring that has none apex;

(2) Find the lowest apex from the three apexes, and if there are two lowest apexes choose the left one as shown in Fig.4b;

(3) Add the chosen apex as the first apex into the ring;

(4) Respectively make connection between the first apex and the two remaining apexes, so that the two connections will be at two different angles to the positive X-axis and the smaller one is made up of the first and the second apexes as shown in Fig.4a;

(5) Add the second apex and the third apex into the ring.

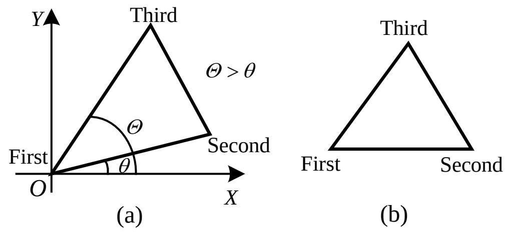

Fig.4 Sort the three apexes of a triangular facet into a ring. (a) Each apex of different height; (b) Two apexes of the same height

After all the triangular facets that need HBS are merged into 3D rings, the merged 3D rings also have to be merged into a series of independent rings. The principles of merging the rings are as follows:

(1) Remove the common border of two adjacent rings that have the same direction;

(2) Rearrange all the remaining borders in the direction that the rings follow as shown in Fig.5.

Fig.5a shows that ring 1 and ring 2 are two adjacent rings and have the same direction. Border 2 of ring 1 and border 3 of ring 2 are removed, and a new ring 1 is achieved as shown in Fig.5b.

The merged rings can be divided into inner-rings and outer-rings. If the outer-ring contains one or more inner-rings, the HBS region covers the area inside the outer-ring but outside the inner-rings, as shown in Fig.6. An HBS region is a 3D surface. A number of separate HBS regions may exit in a part. After all the HBS regions have been identified, the auxiliary triangular facets of the HBS regions will be identified. Extracting auxiliary triangular facets is necessary in generating HBS, because some HBSs are generated from other regions of the part, which are composed of auxiliary triangular facets. The principles of extracting auxiliary triangular facets are as follows:

(1) The projection of the auxiliary triangular facet on XOY plane must be included in the projection of HBS region on the same plane;

(2) The Z-axis coordinates of the three apexes of the auxiliary triangular facet must be less than the Z-axis coordinate of the three apexes of the

corresponding HBS triangular facet, also the normal vector of the auxiliary triangular facet must be upward.

The extracted auxiliary triangular facets must also be merged into auxiliary HBS regions.

Because the radius of the laser beam must be taken into consideration during processing, the HBSs cannot be directly generated from the merged HBS regions. As shown in Fig.7, when processing a ring the laser path must be offset from the outline of the ring, which is operated inwards for outer-rings and outwards for inner-rings. The downward projection of an HBS region contains one outer-ring and none or more inner-rings. As the outline of the cross-section of an HBS region is formed by closed polygons, the compensatory outline should also consist of some closed polygons. In order to get the compensatory outline, the equidistant lines of the outline of the polygons together with the intersections of the equidistant lines should be calculated. Obtained by connecting the intersections, the compensatory outline also contains inner-rings and outer-rings, and there may be intersections between the inner-rings and inner-rings or self-intersections between the outer-rings and inner-rings. After all the intersected rings and self-intersected rings have been removed and all the remaining rings have been rearranged, the compensatory HBS region can be calculated.

EXPERIMENTS AND DISCUSSION

As shown in Fig.1 and Fig.8, five STL models of different shape are selected in this section to demonstrate the efficiency of the above algorithm and the utility of HBS.

A PC with a CPU speed of 2.4 GHz and 512 MB RAM is used for testing the algorithm. Both the time spent in generating HBS and generating support are calculated from this PC. In addition, the support is generated by Magics RP11. Table 1 shows four kinds of experimental data of different STL models, which are the number of triangular facets, the number of HBS regions, the time for generating HBS, and the time for generating support. The curves of the time spent in generating HBS and generating support are shown in Fig.9. It is easy to find that the time for generating HBS is less than that for generating support for the same part. Besides, the larger the number of triangular facets, the more remarkable the advantage of the algorithm in generating HBS.

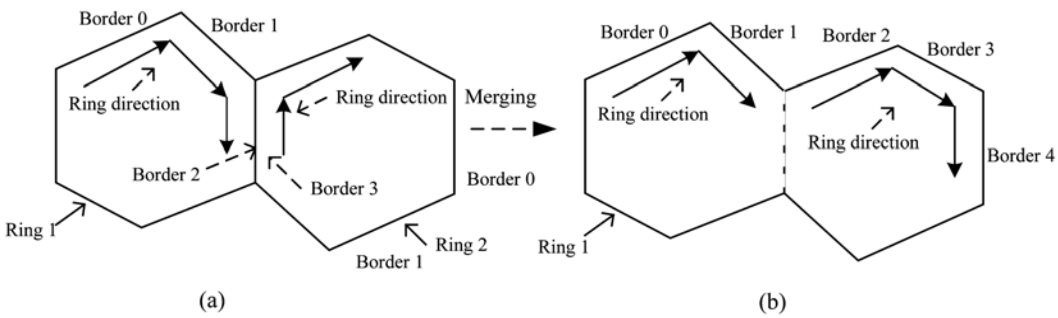

Fig.5 Merge the rings into independent rings. (a) Two adjacent rings; (b) One independent ring

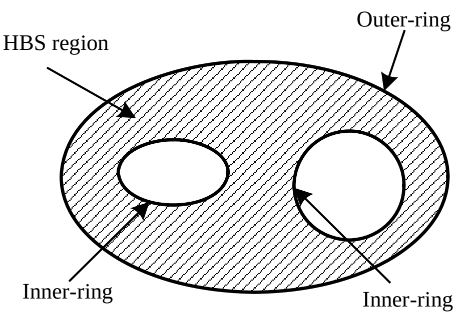

Fig.6 Inner-rings, outer-ring and HBS region

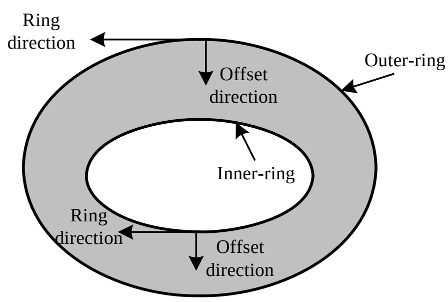

Fig.7 Laser offset of the outline of an HBS region

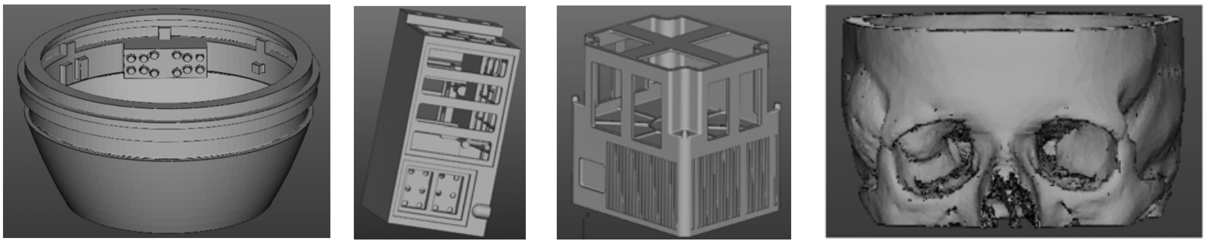

(a) (b) (c) (d)

Fig.8 Example parts. (a) Hood; (b) Shelf; (c) Shell; (d) Skull

Table 1 Experimental data of different STL models

Part	Number		Time (s)	
	Triangular facet	HBS region	Generating HBS	Generating support
Part shown in Fig.1	19442	33	3.8	7.6
Part shown in Fig.8a	55200	23	5.3	15.2
Part shown in Fig.8b	139601	258	103.3	277.7
Part shown in Fig.8c	165574	165	51.2	254.9
Part shown in Fig.8d	353444	97	387.2	872.5

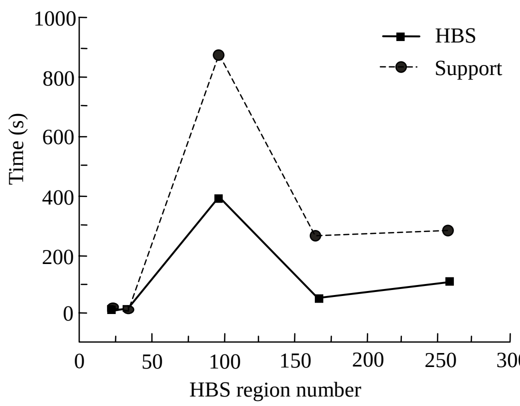

(a)

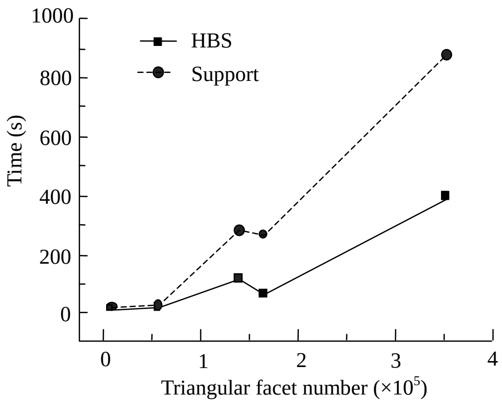

(b)

Fig.9 Curves of the time spent in (a) generating HBS and (b) generating support

The selection of styles and parameters of HBS should follow the three principles below:

(1) The uniformity of the temperature field should be improved as greatly as possible;

(2) The HBS should be easily removed from the part;

(3) The scale of HBS should be as small as possible in order to save processing time.

Two kinds of powders have been chosen for experiment. The first kind of powder is polystyrene (PS). After a number of experiments it can be easily seen that the paths of the laser beam in an HBS region of PS are represented by vertical grid lines. Fig.10 shows the scan lines (vertical grid lines) in the HBS region that is shown in Fig.6. Therefore, dimensional grids of a certain height are selected in HBS for PS. Both the HBSs and the entities are shown in Fig.11.

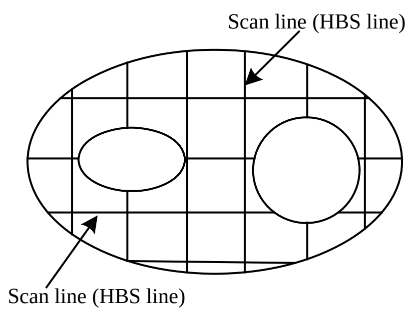

Fig.10 Schematic figure of vertical grid line

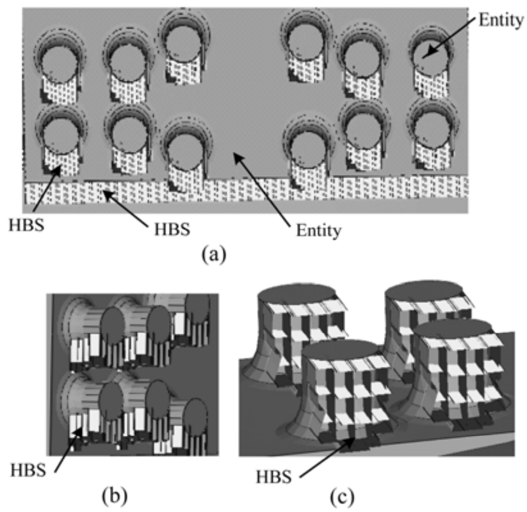

Fig.11 Feature of HBS in PS. (a) Front view; (b) Left view; (c) Bottom and magnified view

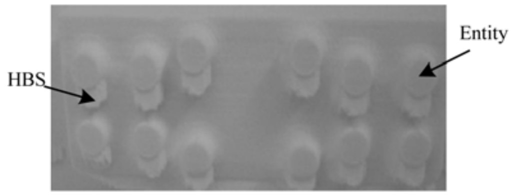

Fig.12 Part processed with HBS

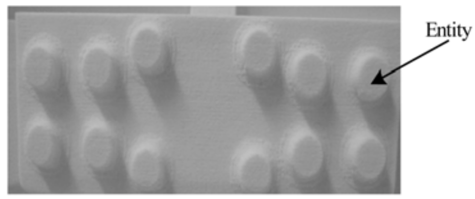

Fig.13 Part cleaned by pneumatic gun

The interval of the dimensional grids should be about 2 mm, the length of the grids equals the width, and the usual height should be about 5 mm. The above parameters are obtained from comparative experiments based on the principles of HBS. These parameters can help to ensure heat equilibrium during SLS processing. What is more, the HBS is very easy to clean out. When the interval is larger than 2 mm, the HBS cannot supply enough bottom heating; when the interval is smaller than 2 mm, the HBS cannot be removed easily. When the grid is shorter than 5 mm, the HBS cannot supply both enough and regular bottom heating. On the other hand, when the grid is higher than 5 mm, it is a waste of processing time and powders. Fig.12 clearly shows the entities of the part and the HBSs. By using the pneumatic gun for powder cleaning, it is easy to clean out HBSs and the powders sticking to the part. As shown in Fig.13, after the powders have been pneumatically cleaned out, the geometrical outline of the part is very precise. Fig.14 shows a part processed with HBS, whose geometrical features are much better than those of the part shown in Fig.2.

The second kind of powder is nylon (Kim and Creasy, 2004; Zarringhalam *et al*., 2006). For the reason that nylon has great contractibility, the part is more likely to warp when the temperature field is non-uniform. If the style of HBS is similar to that of PS, the scale of the grids should be relatively small, so that high uniformity of the temperature field can be ensured. In addition, as a kind of crystalline polymer, nylon is thoroughly melted after being sintered and the molecules of nylon are more firmly bonded together than those of PS. If the HBS of PS style is chosen, which is a continuum and has grids of a relatively small scale, the HBS will be too firmly bonded to the part to be removed. Therefore, HBS should be in a discrete state and be able to provide a uniform temperature field. After a number of experiments, it was concluded that the paths of the laser beam in an HBS region of nylon are represented by a series of circles as shown in Fig.15b. Generally, columns of a certain height are selected in HBS as shown in Fig.15. It is also concluded that the radius of the column is 0.5 mm, the interval of the two columns is 3 mm, and the height of the column is 3 mm. If the radius is larger than 0.5 mm, or the interval is smaller than 3 mm, the HBS will not be removed easily. Whereas if the radius is smaller than 0.5 mm or the interval is larger than 3 mm, the HBS cannot supply enough bottom heating. It is for the same reason that 3 mm is chosen as the height of the column and 5 mm as the height of HBS for PS.

Table 2 shows the contrast in efficiency between the conventional method and the method of automatically adding HBS (Stevinson *et al*., 2006). Fig.16 shows the curves of the time spent in manufacturing parts with and without HBS. It is obvious that manufacturing the part with HBS can save a lot of time.

Fig.14 A well processed part

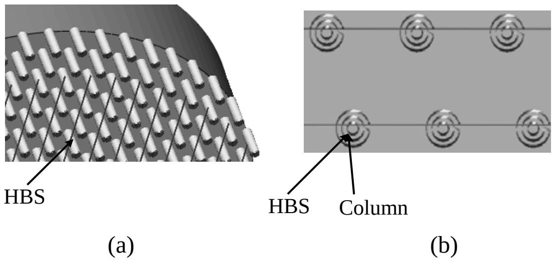

Fig.15 Feature of HBS in nylon. (a) Overall view; (b) Bottom and magnified view

Table 2 Efficiency contrast between the conventional method and the method of automatically adding HBS

Part	Time (h)						Elevated efficiency (%)
	Conventional processing	Conventional post processing	Conventional total processing	Processing with HBS	Post processing with HBS	Total processing with HBS	
Part shown in Fig.1	2.4	6	8.4	2.6	0.2	2.8	200
Part shown in Fig.8a	13.5	10	23.5	13.8	0.3	14.1	67
Part shown in Fig.8b	42.5	50	92.5	45.0	0.5	45.5	103
Part shown in Fig.8c	45.3	7.8	53.1	46.5	0.5	47.0	13
Part shown in Fig.8d	5.3	60	65.3	6.2	1.0	7.2	806

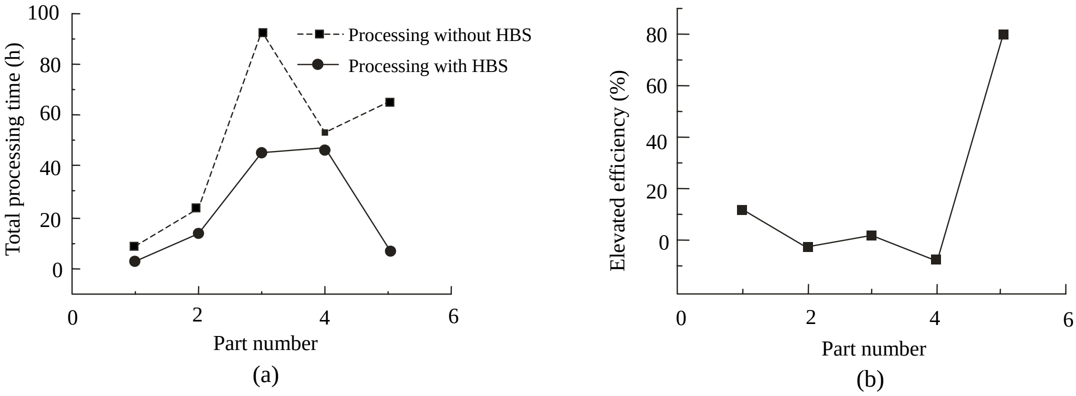

Fig.16 Curves of the time spent in manufacturing parts with and without HBS. (a) Time contrast; (b) Elevated efficiency

CONCLUSION

Some key factors that affect accuracy and quality of the parts have been analyzed in this study. Adding HBS during SLS processing is a new method of solving the thermal imbalance in the build chamber.

The detailed algorithm of automatically generating HBS has been elaborated. The algorithm adopts a recursive method to obtain the triangular facets that need HBS in the STL file. Through tests on several complex STL models, the algorithm exhibits high efficiency.

Because of differences in some characteristics of different polymers, such as crystallizability and contractibility, the style of HBS is varied in order to comply with the three principles of HBS. The features of the paths as well as the parameters in an HBS region have been studied and tested well for PS and nylon.

The higher accuracy the part has, the less time it will take to repair it in post processing using the HBS method than the conventional method. The part processed with HBS has much better accuracy in its shape and size than that without HBS. The parts manufactured with HBS have higher productivity than those without HBS.

References

Ang, B.Y., Chua, C.K., Du, Z.H., 2000. Study of trapped material in rapid prototyping parts. *International Journal of Advanced Manufacturing Technology*, **16**(2):120-130. [doi:10.1007/s001700050017]

Armillotta, A.B.G., 2001. Control of Prototyping Surface Finish through Graphical Simulation. Proceedings of the VII ADM International Conferences, Rimini, Italy, p.17-24.

Chua, C.K., Chou, S.M., Wong, T.S., 1998. A study of the state-of-the-art rapid prototyping technologies. *International Journal of Advanced Manufacturing Technology*, **14**(2):146-152. [doi:10.1007/BF01322222]

Chua, C.K., Gan, J., Du, Z., Mei, T., 2002. Data Structure in Rapid Prototyping and Manufacturing. Database and Data Communication Network Systems, p.367-416.

Dai, K., Shaw, L., 2004. Thermal and mechanical finite element modeling of laser forming from metal and ceramic powders. *Acta Materialia*, **52**(1):69-80. [doi:10.1016/j.actamat.2003.08.028]

Du, Z.Q., Zhou, Z.D., Ai, W., Chen, Y.P., 2007. A linear drive system for the dynamic focus module of SLS machines. *The International Journal of Advanced Manufacturing Technology*, **32**(11-12):1211-1217. [doi:10.1007/s00170-006-0442-5]

Exner, H.H.M., Streek, A., Ullmann, F., Hartwig, L., Regenfu, P., Ebert, R., 2008. Laser micro sintering: A new method to generate metal and ceramic parts of high resolution with sub-micrometer powder. *Virtual and Physical Prototyping*, **3**(1):3-11. [doi:10.1080/17452750801907970]

Guo, K.B., Zhang, L.C., Wang, C.J., Huang, S.H., 2007. Boolean operations of STL models based on loop detection. *International Journal of Advanced Manufacturing Technology*, **33**(5-6):627-633. [doi:10.1007/s00170-006-0487-5]

Hardro, P.J., Wang, J., Stucker, B.E, 1998. A Design of Experiment Approach to Determine the Optimal Process Parameters for Rapid Prototyping Machines. Proceedings of the Joint Conference of the Fifth International Conference on Automation Technology and the 1998 International Conference of Production Research, Taipei.

Kim, J., Creasy, T.S., 2004. Selective laser sintering characteristics of nylon 6/clay-reinforced nanocomposite. *Polymer Testing*, **23**(6):629-636. [doi:10.1016/j.polymertesting.2004.01.014]

Kochan, D., Chua, C.K., Du, Z.H., 1999. Rapid prototyping issues in the 21st century. *Computers in Industry*, **39**(1):3-10. [doi:10.1016/S0166-3615(98)00123-7]

Kolossov, S., Boillat, E., Glardon, R., Fischer, P., Locher, M., 2004. 3D FE simulation for temperature evolution in the selective laser sintering process. *International Journal of Machine Tools & Manufacture*, **44**(2-3):117-123. [doi:10.1016/j.ijmachtools.2003.10.019]

Maeda, K., Childs, T.H.C., 2004. Laser sintering (SLS) of hard metal powders for abrasion resistant coatings. *Journal of Materials Processing Technology*, **149**(1-3):609-615. [doi:10.1016/j.jmatprotec.2004.02.024]

Majewski, C.E., Hobbs, B.S., Hopkinson, N., 2007. Effect of bed temperature and infra-red lamp power on the mechanical properties of parts produced using high-speed sintering. *Virtual and Physical Prototyping*, **2**(2):103-110. [doi:10.1080/17452750701520915]

Ming, L.W., Gibson, I., 2006. Experimental investigation of ink on powder used for selective laser sintering. *Journal of Materials Processing Technology*, **174**(1-3):91-101. [doi:10.1016/j.jmatprotec.2005.04.094]

Qi, B., Himmer, A.P., Gordon, L.M., Yang, X.D.V., Dickensheets, L.D., Vitkin, I.A., 2004. Dynamic focus control in high-speed optical coherence tomography based on a microelectromechanical mirror. *Optics Communications*, **232**(1-6):123-128. [doi:10.1016/j.optcom.2004.01.015]

Stevinson, B., Bourell, D.L., Beaman, Jr.J.J., 2006. Dimensional stability during post-processing of selective laser sintered ceramic performs. *Virtual and Physical Prototyping*, **1**(4):209-216. [doi:10.1080/17452750601107003]

Wang, R.J., Wang, L.L., Zhao, L.H., Liu, Z.J., 2007. Influence of process parameters on part shrinkage in SLS. *International Journal of Advanced Manufacturing Technology*, **33**(5-6):498-504. [doi:10.1007/s00170-006-0490-x]

Williams, J.D.D.C., 1998. Advances in modeling the effects of selected parameters on the SLS process. *Rapid Prototyping Journal*, **4**(2):90-96. [doi:10.1108/13552549810210257]

Yang, H.J., Hwang, P.J., Lee, S.H., 2002. A study on shrinkage compensation of SLS process by using the Taguchi method. *International Journal of Machine Tools and Manufacture*, **42**(11):1203-1212. [doi:10.1016/S0890-6955(02)00070-6].

Zarringhalam, H., Hopkinson, N., Kamperman, N.F., de Vlieger, J.J., 2006. Effects of processing on microstructure and properties of SLS nylon 12. *Materials Science and Engineering*, **435-436**(A):172-180. [doi:10.1016/j.msea.2006.07.084]